Orientation-Dependent Interactions in Polymer Systems. 5. Thermotropic Liquid Crystalline Transition of Tri-*O*-heptylcellulose

Akihiko Takada,† Takeshi Fukuda,* Junji Watanabe,‡ and Takeaki Miyamoto

Institute for Chemical Research, Kyoto University, Uji, Kyoto 611, Japan

Received August 9, 1994; Revised Manuscript Received December 22, 1994[⊗]

ABSTRACT: Fairly narrow fractions of tri-*O*-heptylcellulose (THC) covering a wide range of degrees of polymerization (DP) were prepared and studied by viscometry and light scattering to determine the wormlike model parameters of the polymer to be $q = 43.2 \exp(-0.0050T)$ nm and $M_L = 880$ nm^{-1}, where q is the persistence length, M_L is the shift factor, and T is the absolute temperature. The same fractions were studied with their thermal properties to determine the anisotropic−isotropic transition temperature T_i and transition entropy ΔS as a function of DP. Both T_i and ΔS increased with increasing DP to approach a limiting value for large enough DP. These trends were favorably compared with the predictions of the statistical models with the above-noted parameter values. It was shown that the main factor that causes the thermotropic transition and the chain-length dependence of T_i in bulk THC is the temperature-dependent flexibility of the polymer.

Introduction

The thermotropicity or temperature-induced order−disorder orientational transition in semiflexible polymers can originate in two different mechanisms. One is related to the intermolecular energetic (soft) interaction. Since the relative importance of the energetic term decreases with increasing temperature, the ordered phase stabilized by an energetic effect will become unstable at high enough temperature. This mechanism is common to all types of mesogenic compounds including low-mass rodlike molecules and semiflexible polymers. The other mechanism, originally proposed by Krigbaum, Ciferri, and co-workers, involves the variation of molecular flexibility with temperature.[1,2] Namely, as the temperature is raised, a chain molecule will become more flexible, increasing its conformational entropy and thus making it more difficult to take the oriented conformation in the ordered phase. Therefore, the ordered phase stable at low temperatures will eventually become unstable at high temperatures, irrespective of the ordered phase being stabilized by a soft or a hard (excluded volume) interaction. This mechanism is unique to semiflexible polymers but is not characteristic of low-mass rigid mesogens.

In a previous paper,[2] we have discussed the nematic−isotropic transition behavior of semiflexible polymers in the bulk on the basis of several sets of simple statistical models. One of the main results obtained therein was the characteristic dependence of the transition temperature on chain length, which originates in the temperature dependence of chain flexibility. Also the latent heat of phase transition was predicted to depend on chain length in a characteristic fashion.

In this work, we have attempted to make a comparison of these predictions with experimental data. For this purpose, we have chosen tri-*O*-heptylcellulose (THC) as a model polymer. This polymer forms a (chiral) nematic phase in the bulk in a fairly wide temperature range.[3,4] It has no strongly polar groups and is soluble in a number of common solvents. This work includes the preparation, fractionation, and molecular characterization of THC as well as detailed measurements of the thermotropic properties. Such comprehensive study has been rare in the literature.

Experimental Section

Preparation of Tri-*O*-heptylcellulose (THC). Two methods were attempted to prepare THC. One method uses cellulose as a starting material. A commercially obtained cellulose (Avicel PH301, Asahi Chemical Industries, Japan) and a regenerated cellulose with a relatively low degree of polymerization (DP), which was obtained by hydrolyzing[3] a cellulose triacetate (CTA) with a nominal DP of 210 (Daicel Chemical Industries, Japan), were used. The other method starts with CTA. A commercially obtained CTA with a nominal DP of 360 (Asahi Chemical Industries) was used as a starting polymer in the second method.

In a typical procedure based on the first method, 5 g of cellulose was dissolved in the solvent system composed of SO_2 (6.0 g), diethylamine (9.5 g), and dimethyl sulfoxide (500 mL), and 46 g of powdered sodium hydroxide was added as an activator.[5a] To the suspension thus obtained was added dropwise at room temperature a 7-fold excess, relative to the number of moles of OH groups, of heptyl bromide. The mixture was stirred at 60 °C for 12 h. After cooling to room temperature, it was poured into a 10-fold excess of methanol to precipitate the polymer, which was successively purified by using a tetrahydrofuran (THF)/methanol system. This gave a heptylcellulose with a degree of substitution (DS) of about 2.8 or larger. To achieve full substitution, the polymer (5 g) was then dissolved in dry THF (500 mL), to which a 1 N solution of sodium naphthalene in THF was added dropwise under a nitrogen atmosphere until the blue color of the sodium naphthalene complex remained undestroyed. The system was stirred for 30 min at room temperature, to which a large excess of heptyl bromide was added, and the reaction was allowed to proceed at 50 °C for 12 h.[5b] The product was recovered and purified as described above.

The second method, originally suggested by Kondo et al.,[6] is simpler. To the homogeneous solution of CTA (10 g) in dimethyl sulfoxide (600 mL) were added powdered sodium hydroxide (64 g) and then heptyl bromide (290 g), and the reaction was allowed to proceed at 60 °C for 4 h and then at 90 °C for 30 min. It was suggested that the presence of a small amount of water in the system is important in this deacety-

† Present address: Faculty of Human Life Science, Osaka City University, Sugimoto, Sumiyoshi-ku, Osaka 558, Japan.
‡ On leave from the Department of Polymer Chemistry, Tokyo Institute of Technology, Ookayama, Meguro-ku, Tokyo 152, Japan.
⊗ Abstract published in *Advance ACS Abstracts,* March 15, 1995.

0024-9297/95/2228-3394$09.00/0

Chart 1. Structure of Tri-*O*-heptylcellulose (THC)

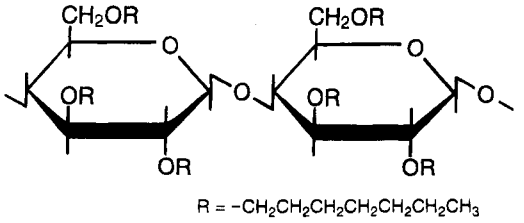

lation–alkylation reaction.[6] We deliberately added no water to the system, since it was found to cause significant degradation of the main chain. We presume that a catalytic amount of water possibly present in the usual (not perfectly dried) system suffices for the reaction to proceed. After the system was cooled to room temperature, 500 mL of water and then 500 mL of chloroform were added to it to extract the polymer. The chloroform phase was washed three times with water, concentrated, and then poured into a large excess of methanol. The recovered polymer was purified by reprecipitation with a THF/methanol system.

Both of the two methods gave THC, i.e., fully heptylated cellulose (Chart 1). Actually, a proton NMR analysis showed that the DS values of the products are 3.0 with an analytical uncertainly of ±0.1, in all cases. The infrared spectra of the products showed virtually no hydroxyl-related absorption band around 3400 cm^{-1}, which also confirmed full substitution.

Fractionation. Each THC product was subjected to the precipitation fractionation by using benzene as a solvent and methanol as a nonsolvent, and divided into six to eight fractions. The weight- to number-average molecular weight ratios, M_w/M_n, of the fractions as estimated by gel permeation chromatography (GPC; see below) ranged from about 1.3 to 1.4, while those of the original THCs were about 2.0. Out of these fractions, five appropriate ones were selected and subjected to a further fractionation by use of GPC. A Toyo Soda semipreparative GPC Model HLC-827, Japan, was employed for this purpose. The gel columns used were Toyo Soda TSKG2000HG8, G3000HG8, and MGHG6. A flow rate of 6.0 mL/min was maintained with chloroform as eluent. Each fraction was divided into six parts or more in this way.

Molecular Characterization. Light-scattering measurements were made on a Fica automatic photometer Model 50, France. The apparatus was calibrated with benzene, whose Rayleigh ratio U_u and depolarization ratio ϱ_u at 25 °C were taken to be 46.5 × 10^{-6} and 0.42, respectively.[7] Most measurements were made at 23.0 °C in the angular range from 30 to 150°. The V_v intensities from bromobenzene solutions were determined. The effect of anisotropic scattering was negligibly small in all studied cases. The refractive index increment $\partial n/\partial c$ of THC in bromobenzene at 23.0 °C was determined to be −0.117 mL/g by means of a Union Giken differential refractometer RM102, Japan. The value of $\partial n/\partial c$ may be regarded as constant in the studied molecular weight range. Figure 1 shows the Zimm plot for a THC/bromobenzene system. The M_n values of a few low-mass samples were determined on a Corona vapor pressure osmometer Model 117, Japan, with benzene as solvent.

A GPC analysis was made with a Shimadzu high-performance liquid chromatogram HLC-802UR, Japan, installed with TSK G4000HG and 5000HG gel columns. THF was used as eluent and a flow rate of 1.2 mL/min was maintained.

Viscosities of bromobenzene solutions were determined at 30.0 °C with a Ubbelohde viscometer. The intrinsic viscosity $[\eta]$ was evaluated as a common intercept at $c = 0$ of the η_r/c vs c and the $(\ln \eta_r)/c$ vs c plots. No correction for the kinetic and/or non-Newtonian effects seemed necessary.

Thermal Transitions. Differential scanning calorimetry (DSC) was conducted on a Rigaku Denki Model DSC-8230, Japan, at a constant heating/cooling rate of 10 °C/min under a nitrogen flow. The anisotropic–isotropic transition temperature (isotropization temperature) T_i was determined by measuring the intensity of the light transmitted through crossed polars. A Nikon microscope Model Optiphoto-Pol, Japan, equipped with a photodiode detector and a Mettler hot stage Model FP-82 along with a temperature controller Model FR-80 were used for this purpose. The polymer sample was placed between two pieces of glass with a Teflon spacer of about 75 μm thickness. It was confirmed that heating rates less than about 1 °C/min produce essentially the same result, and hence the measurements were made at 1 °C/min.

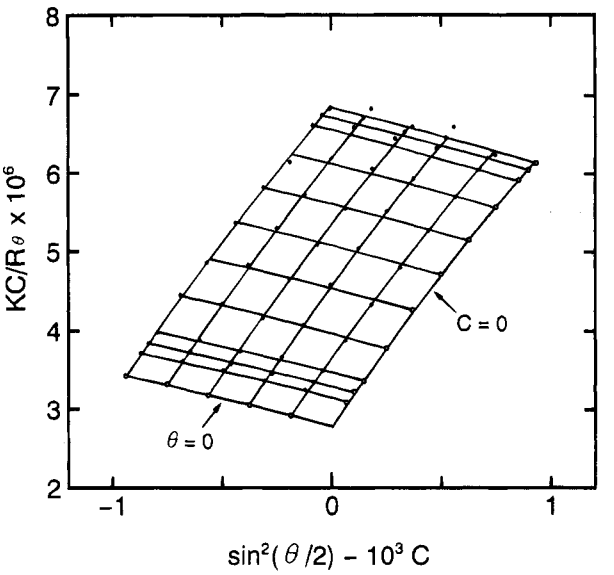

Figure 1. Zimm diagram for THC fraction F2 in bromobenzene at 23.0 °C.

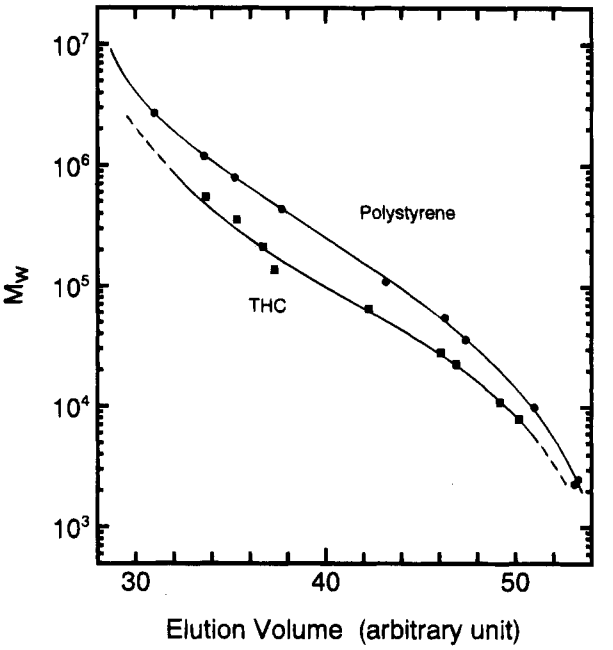

Figure 2. GPC calibration curves for THC and standard polystyrenes in tetrahydrofuran.

Results and Discussion

Molecular Characterization. Nine of the prepared THC fractions were studied by light scattering to determine their M_w values. Figure 2 shows the GPC calibration curve, in which log M_w is plotted against the peak elution volume. For comparison, the curve obtained with standard polystyrenes in the same solvent THF is also shown in the figure, indicating a large difference from the THC curve. In a strict sense, the THC calibration curve is not rigorously correct, since the elution volume corresponding to a given value of M_w is generally different from that at the elution peak,

Table 1. Characteristics of Tri-*O*-heptylcellulose Samples

code	$10^{-4}M_w$[a]	M_w/M_n[b]	$[\eta]$, mL/g	T_i, °C	ΔH, kcal/mol of glucose
F1	55.1	1.31	422	154	0.514
F2	35.8	1.30		154	0.521
F3	28.5[b]	1.34		153	
F4	21.4	1.15	211		
F5	13.8	1.18	140		
F6	6.50	1.24	76.8		
F7	4.01[b]	1.07		134	0.398
F9	2.81	1.09		129	0.342
F10	2.27	1.09	24.3	116	0.275
F12	2.05[b]	1.15		120	0.230
F13	1.51[b]	1.11		108	0.166
F15	1.10	1.16	12.6	92	0.055
F16	0.939[c]	1.22	9.7	72	
F17	0.794	1.17		77	~0[d]
F18	0.508[c]	1.16	6.1		

[a] By light scattering. [b] By GPC. [c] Estimated by vapor pressure osmometry and GPC. [d] No obvious peak observed by DSC.

unless the sample is monodisperse. We have proposed an iterative method to correct the curve for this difference.[8] In the present case, however, the correction was unimportant, because the molecular weight distributions of the THC fractions were fairly narrow. A calibration curve covering a low-mass range of THC was also constructed for a different column system on the basis of the M_n values determined by vapor pressure osmometry.[3] This was used to characterize some low-mass fractions. Table 1 summarizes the molecular weight values of the samples. The values of M_w/M_n, estimated by the mentioned GPC method, ranged from about 1.1 to about 1.3, in all cases. The M_w values of samples F3, F7, F12, and F13 were estimated by the GPC method, while those of F16 and F18 were evaluated from the vapor pressure M_n values along with the GPC M_w/M_n values.[3]

In order to characterize the conformational properties of THC, the values of $[\eta]$ of selected fractions were determined in bromobenzene at 30.0 °C, as reported in Table 1. Figure 3 shows the plot of log $[\eta]$ vs log M_w, where we see that the data points do not form a straight line but a sigmoidal curve, as is typical of a semiflexible polymer. This suggests that THC may be modeled by the Kratky–Porod (KP) wormlike chain. The wormlike cylinder model, whose $[\eta]$ was formulated by Yamakawa et al.,[9,10] is characterized by three parameters, i.e., the persistence length q, the diameter D of the cylinder and the shift factor $M_L = M/L$, where L is the contour length of the chain. Since the theory is not very sensitive to D, we make an independent estimate of it according to the relation[11]

$$v = (\pi N_A/4)(D^2/M_L) \tag{1}$$

where v is the partial specific volume of the polymer at zero concentration. For v, we adopt the relation $v = 0.84 \pm 0.024n$ (mL/g) established for tri-*O*-alkylcellulose in benzene at 30.0 °C, where n is the carbon number of the alkyl side chain ($2 \le n \le 10$).[12] If the monomeric projection h of THC along the chain axis is assumed to be 0.517 nm, which is correct for the trans conformation[13] and is indeed consistent with the present experimental data (see below), D is estimated to be 1.37 nm. Actually, we compared the experimental data with the touched-bead wormlike (TBW) model formulated by Yoshizaki et al.,[14] which has a wider range of applicability than the wormlike cylinder model.[9,10] It was suggested that the two models are well correlated with each other by setting $D = 0.74d_b$, where d_b is the diameter of the bead.[28] The $[\eta]$ of the TBW model has been given as a sum of the two terms

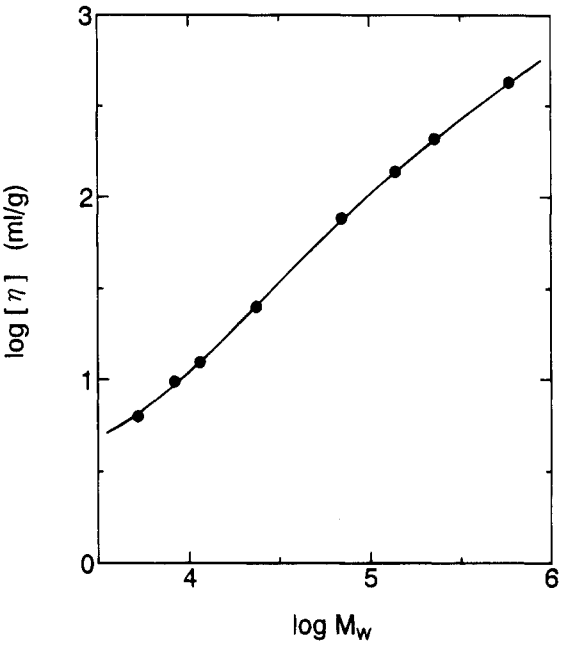

Figure 3. Plot of log $[\eta]$ vs log M_w for THC in bromobenzene at 30.0 °C (circles). The curve represents the touched-bead wormlike model with q = 9.7 nm, M_L = 880 nm^{-1}, and d_b = 1.85 nm (D = 1.37 nm).

$$[\eta] = [\eta]_{KR} + [\eta]_E \tag{2}$$

where $[\eta]_E$ is the Einstein viscosity of a bead and $[\eta]_{KR}$ is the Kirkwood–Riseman solution for the $[\eta]$ of the wormlike or KP chain:

$$[\eta]_{KR} = \Phi_\infty \frac{(6\langle S^2\rangle_{KP})^{3/2}}{M} \Gamma_{KP} \tag{3}$$

In eq 3, $\Phi_\infty = 2.87 \times 10^{23}$ mol^{-1} and $\langle S^2\rangle_{KP}$ is the mean-square radius of gyration of the (unperturbed) KP chain given by[15]

$$\langle S^2\rangle_{KP} = \left(\frac{qL}{3}\right)\left[1 - \frac{3q}{L} - \frac{6q^2}{L^2} - \frac{6q^3}{L^3}(1 - e^{-L/q})\right] \tag{4}$$

and Γ_{KP} is a known function of L/q and d_b/q.[14]

The full curve in Figure 3 represents the best fit TBW model, calculated with q = 9.7 nm and M_L = 880 nm^{-1} along with the fixed D value of 1.37 nm. The experimental data that covers 2 orders of magnitude in M_w are well reproduced by the model. This value of M_L corresponds to an h value of 0.52 nm, which coincides with the monomeric projection for the trans conformation, as already noted. If we make best-fit calculations with the fixed h value of 0.517 nm (M_L = 884 nm^{-1}), we obtain q = 9.5 nm and D = 1.5 nm as optimum q and D values with the associated $[\eta]$ vs M curve almost indistinguishable from the one shown in Figure 3. Thus the set of parameter values estimated above should be sufficiently unique. We also analyzed the $[\eta]$ data according to the linearization method proposed by Bushin et al.[16] and Bohdanecký[17] and obtained q = 8.4 nm and M_L = 780 nm^{-1} with the fixed D of 1.37 nm (Figure 4). These q and M_L values are about 15% smaller than those obtained above by the direct curve-

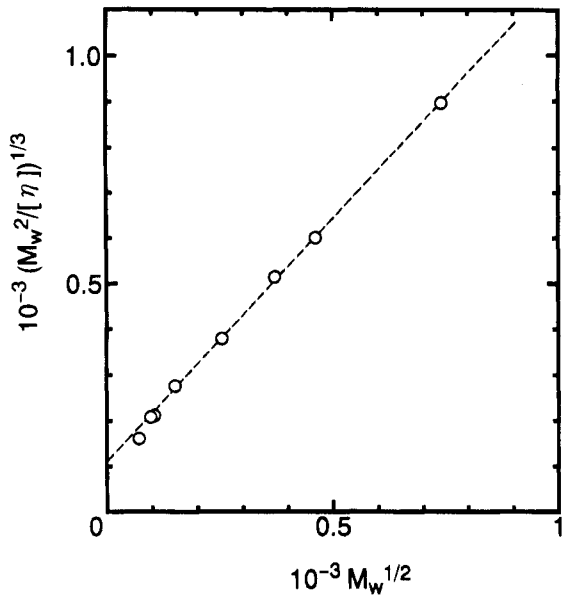

Figure 4. Bohdanecký plot for the data given in Figure 3.

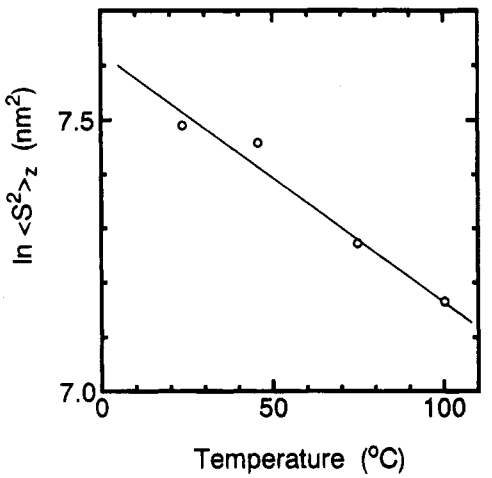

Figure 5. Plot of log $\langle S^2\rangle_z$ vs T for THC in bromobenzene.

fitting method, while the ratios q/M_L estimated by the two methods are nearly the same. In the linearization method, the slope and the intercept at $M^{1/2} = 0$ of the linearized curve are predominated by the ratio q/M_L and M_L, respectively. Hence data points for low-mass samples play a dominant part in determining M_L and also q, since the slope or q/M_L is rather insensitive to them. We would prefer the direct curve-fitting method to the linearization method, in the latter of which statistical weights can be uneven.

The temperature coefficient of q was estimated by conducting light-scattering measurements on a THC sample at several temperatures between 23 and 100 °C. For this purpose, we chose sample F2, because its molecular weight ($M_w = 3.58 \times 10^5$) is large enough that $\langle S^2\rangle$ can be accurately determined, but still small enough that the intramolecular excluded volume effect is unimportant (see below). Figure 5 shows the logarithm of z-average mean-square radius $\langle S^2\rangle_z$ as a function of temperature T. The value of $\langle S^2\rangle$ of a KP chain of this size and flexibility may be given by the first two terms on the right-hand side of eq 4, from which we obtain the following approximate relation:

$$\frac{\partial \ln q}{\partial T} \cong \frac{\partial \ln \langle S^2\rangle_z}{\partial T}\left(1 + \frac{3q}{L}\right) \qquad (5)$$

With the observed slope $\partial \ln \langle S^2\rangle_z/\partial T$ and the known values of q (=9.7 nm at 30 °C) and L (=M_w/M_L, M_L = 880 nm^{-1}), we finally obtain

$$q = q_0 \exp(-\beta T)\ (\text{nm}) \qquad (6)$$

with $q_0 = 43.2$ nm and $\beta = 5.0 \times 10^{-3}$ K^{-1}.

In order to check the consistency of the viscometric and light-scattering results, we set $L = M_w/M_L$, and by using eqs 4 and 6, we calculate $\langle S^2\rangle^{1/2}$ of sample F2 at 23 °C to be 35.2 nm. On the other hand, if the observed $\langle S^2\rangle_z^{1/2}$ value of 42.3 nm at 23 °C is corrected for the sample polydispersity by multiplying it by a factor $(M_w/M_z)^{1/2}$ with M_z/M_w being 1.37 by GPC, we obtain a radius value of 36.1 nm, which is in good agreement with the calculated value. Another comment concerns the intramolecular excluded volume effect. According to Norisuye and Fujita,[18] the excluded volume effect on the $\langle S^2\rangle$ of semiflexible polymers becomes appreciable when the number of Kuhn segments $n_K = L/2q$ exceeds about 50. For sample F2, n_K never exceeds about 30 below 100 °C, according to the above-obtained results. At 30 °C, where the $[\eta]$ analysis was made, the n_K of the highest M_w sample (F1) is about 30, and therefore we may assume that our $[\eta]$ and $\langle S^2\rangle$ data are essentially free from the excluded volume effect. It is also noted that the correction of the $[\eta]$ data for sample polydispersity[19] was unimportant. This is because the exponent a in the relation $[\eta] = KM_w^a$ was reasonably close to 1.0 in the studied range of M_w, and also because the molecular weight distributions of the samples were fairly narrow.

Cellulose derivatives whose persistence length was accurately determined are not many, but the literature data indicate that the q of cellulose derivatives ranges from several nanometers to a few tens of nanometers, depending on the substituent, the degree of substitution, solvent, and temperature.[20] Cellulose tricarbanilate (CTC) and cellulose trinitrate (CTN) are among the fully substituted derivatives that have been studied extensively. Danhelka et al.[21] have analyzed the $[\eta]$ data on CTC by the Bohdanecký method[17] to estimate q to be 9.7 nm in THF at 25 °C and 10.2 nm in acetone at 25 °C. The $[\eta]$ data on CTN[22] similarly analyzed gave q = 14.5 nm in acetone at 20 °C.[17] The temperature coefficient β, which is equivalent to $-\mathrm{d} \ln C_\infty/\mathrm{d}T$ with C_∞ being the characteristic ratio for infinitely long chains, has been reported to be around 6×10^{-3} K^{-1} for many cellulose derivatives including CTC[21] and CTN.[23] Thus the value of q and β found here for THC are typical, rather than exceptional, of cellulose derivatives.

Anisotropic–Isotropic Transition in Bulk THC. Among important characteristics of lyotropic liquid crystals is the formation of a biphasic region in which anisotropic and isotropic phases coexist.[24] A biphasic region can also occur in a solvent-free system when the chain length is not large enough and the chain-length distribution is not ideally narrow. This is shown in Figure 6, where the intensity of the light transmitted through crossed polars is plotted as a function of temperature. The broken curve in the figure is for an unfractionated THC ($M_w \cong 1.76 \times 10^4$, $M_w/M_n \cong 1.81$), showing a very wide region of transition. This sample is observed to be fully birefringent at low temperatures ($T < 70$ °C), but as the temperature is raised, the intensity gradually decreases, indicating the emergence and growth of dark isotropic domains. At about 130 °C, the sample entirely ceases to be birefringent. On the

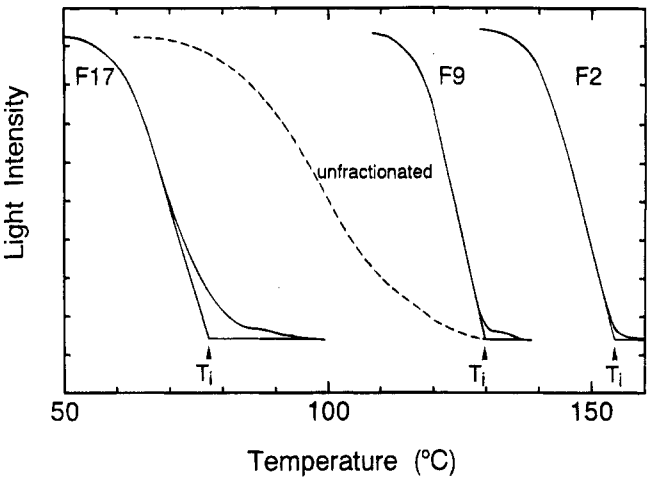

Figure 6. Plot of light intensity vs T for THC fractions (solid curves) and an unfractionated THC (broken curve); heating rate = 1 °C/min.

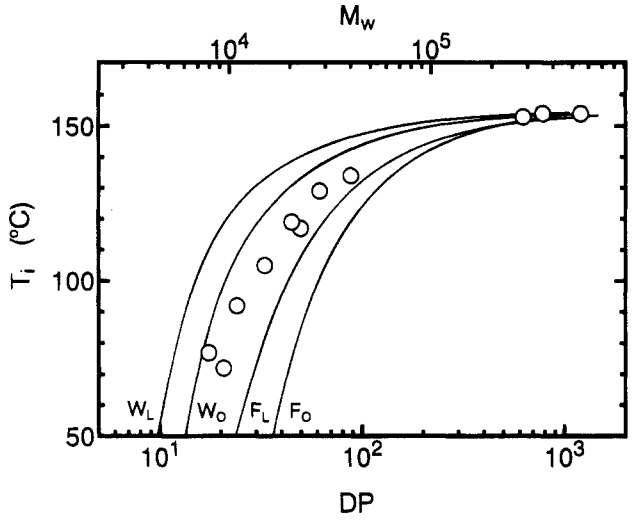

Figure 7. Plot of T_i vs DP for THC fractions (circles). The curves were calculated by the models indicated in the figure (see for details the subsection Comparison with Theory).

other hand, the transition region for fractionated samples or those with a sufficiently large DP is fairly narrow. These behaviors arise from the fact that the isotropization temperature T_i depends on DP in such a manner that T_i rapidly increases with DP for small DP, but gradually levels off approaching a constant value for sufficiently large DP. This is shown in Figure 7, where T_i was determined for the fractionated samples as the temperature at which the tangent line passing through the inflection point of the intensity curve intersects with the horizontal line of the isotropic phase with virtually zero intensity (cf. Figure 6). Perhaps T_i could be defined differently, but we have adopted the mentioned definition because of the good reproducibility of the data thus obtained.

Figure 8 shows the DSC thermograms observed in the heating mode. A clear endothermic peak is observed for high-DP fractions, but the peak becomes less and less clear as DP decreases. The reason why the peaks for low-DP fractions become unclear is 2-fold. First, the enthalpy of transition itself becomes smaller as DP decreases (see below). Second, the span of the transition region becomes larger due to the DP dependence of T_i, for one thing, and to the sample polydispersity, for another. In fact, the DSC thermogram for the unfractionated sample given in Figure 6 is too broad and

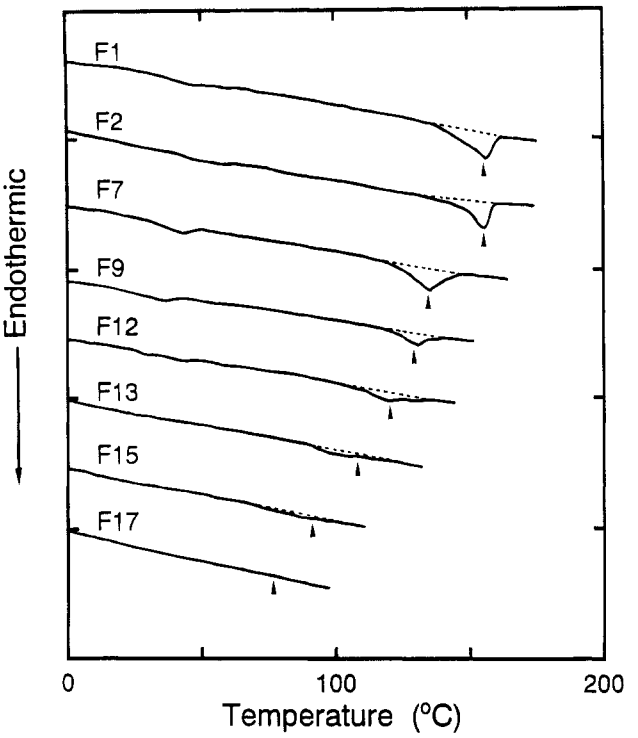

Figure 8. DSC thermograms for THC fractions; heating rate = 10 °C/min. The arrowhead indicates the isotropization temperature T_i determined by the optical method (see text).

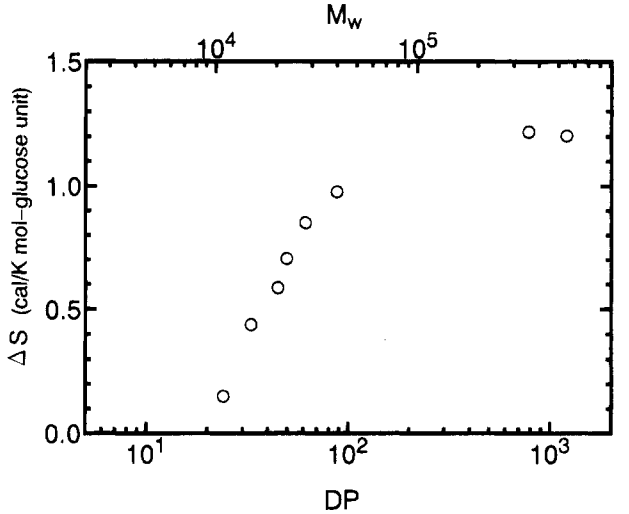

Figure 9. Plot of ΔS vs log DP for THC fractions; ΔS in unit of cal/(K·mol of glucose unit).

shallow to be recognized as an endothermic peak. Adequate fractionation of a sample is essential in this regard, too. The arrowhead attached to each thermogram indicates the T_i photomicroscopically obtained above. The DSC and photomicroscopic results are not perfectly consistent because of the difference in the heating rate (see above), but it is clear that the DSC peaks correspond to the anisotropic–isotropic transition. The enthalpies of isotropization ΔH calculated from the peak areas are presented in Table 1. Figure 9 shows the transition entropy $\Delta S = \Delta H/T_i$ as a function of DP. Interestingly, ΔS decreases with decreasing DP when DP is small.

Comparison with Theory. In the previous work, we discussed the nematic–isotropic transition behavior of semiflexible polymers by using four sets of simple models, referred to as the F_O, F_L, W_O, and W_L models,

respectively.[2] Here F and W denote the modified freely jointed chain and the wormlike chain, respectively, both being characterized by the persistence length q and the contour length L in addition to the diameter D. The subscripts O and L refer to the Onsager-type and the lattice models, respectively, used to account for the hard interaction. The Maier–Saupe-type soft interaction was also taken into account. Since we know the values of $q(T)$ (eq 6), M_L (=880 nm^{-1}), and D (=1.37 nm) for THC in bromobenzene, we can now compare the experiments with the predictions of the models, under the assumption that the molecular parameter values remain unchanged in the solvent-free system.

Figure 7 indicates that the T_i of long enough THC is about 154 °C or T_∞ = 427 K where the axial ratio of the persistent segment, $x = q/D$, is estimated as x_∞ = 3.7. With this value in Figure 3 in ref 2, the energy parameter B^* at T_∞ is evaluated to be 0, 0.28, 0.35, and 0.65 for the F_O, F_L, W_O, and W_L models, respectively. Since, by definition, B^* is inversely proportional to T, the value of B^* at a given temperature T_i is obtained from $B^*(T_i) = (T_i/T_\infty)B^*(T_\infty)$, with which, together with the known value of $x(T_i)$, eq 20 in ref 2 can be solved for m and hence DP. The solid curves in Figure 7 were computed in this way for the respective models. Clearly, both the shape and location of the observed T_i vs DP curve are well reproduced by the models. More specifically, the F_L and W_O curves describe the data particularly well, while the F_O and W_L curves give a poorer description. This analysis did not take into account the effect of sample polydispersity on the transition temperature. A preliminary calculation indicates that this effect is not totally insignificant even for the studied THC fractions, most of which have an M_w/M_n ratio around 1.1. It is expected that the T_i values of ideally monodisperse polymers would be situated, especially for shorter polymers, somewhat below the data points given in the figure, coming closer to the F_L curve. The values of B^* estimated by the F_L and W_O models are rather small (see above), suggesting that the THC mesophase is stabilized mainly by the hard interaction with some support by the soft interaction. We cannot conclude this without any information about the precision of the models, but the result of thermal analysis is not in conflict with this (see below). Aside from these details, the general success of the models is interpreting the trend of the observed T_i vs DP curve evidences that the thermotropicity of THC originates in the temperature-dependent flexibility of the polymer.

The transition entropy ΔS of THC with a large DP was found to be about 1.2 cal/(K·mol of glucose unit) (a similar value, 1.0 cal/(K·mol), has been observed for tris-*O*-(butoxyethyl)cellulose, TBC).[25] This value corresponds to about 10 cal/(K·mol of persistent segment). Values of ΔS for low-mass rodlike compounds are, in most cases, smaller than 1 cal/(K·mol), and, in this regard, the THC (and TBC) value may be unusually large. More importantly, ΔS of THC rapidly decreases with decreasing DP, seemingly approaching zero or a very small value for short chains (Figure 9). This would indicate two things. First, the soft interaction in this system, if any is present, must be very small (or at least of a usual level), since the magnitude of the soft interaction should be essentially independent of DP, and actually the short THCs show nearly zero ΔS. Second, the characteristic DP dependence of ΔS implies that it is related to the conformational change of THC at transition. We have illustrated this for the W_O and W_L

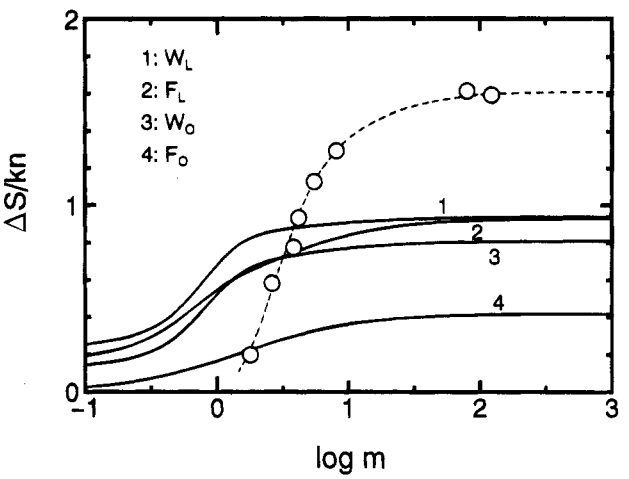

Figure 10. Plot of $\Delta S/nk$ vs log m for THC fractions (circles). The curves were estimated by the models (see text).

models in Figure 8 in ref 2, where we see that the theoretical curves well reproduce the trend of the experimental result given in this work. In that calculation, however, the persistence length was assumed to, very like $q \sim T^{-1}$ or $-T(\partial \ln q/\partial T) = \beta T = 1$, to be consistent with the wormlike model.[26] The value of β observed for THC is about twice as large as this, and in this regard, THC, like many other semiflexible polymers,[2] is not well represented by the wormlike model. In fact, the theoretical values of ΔS_C, i.e., the part of ΔS arising from the conformational change, are much too small to explain the experimental results. In this situation, we are tempted to use, at the sacrifice of internal consistency, the relation suggested previously[2]

$$\Delta S/nk = B^*\eta^2 + (\beta T_i \sigma_\infty/x_\infty)h(m) \qquad (7)$$

with βT_i adjusted so as to agree with the experimental value. In this equation, the order parameter η, the constant σ_∞, and the function h of $m = L/q$ as well as B^* are calculable for each model, given the experimental value of x_∞.[2] The number of submolecules, $n = (M/M_L D)$, is related to the DP of THC by n = 0.38DP. In Figure 10, the $\Delta S/nk$ vs log m curves calculated in this way are compared with the experimental data. Excepting the F_O curve, the calculated curves explain 50–60% of the observed ΔS for large m and reproduce the main feature of the experimental curve.

However, there is still a large difference between theory and experiment. This may indicate inadequacy of the chain models, as already suggested. Alternatively, one may assume the occurrence of some ordering of the *flexible* alkyl side chains. A unit submolecule of THC has as many as eight side chains, and even if the contribution of the individual side chains may be small, their total effect can be large. Ordering of flexible chains in an anisotropic excluded-volume field has been the subject of previous work.[27–29] The observed trend that ΔS approaches zero for short chains poses a new question seemingly difficult to answer along this line, however. Interesting in connection with this is the work of Bhadani et al.,[30] who carried out a detailed analysis of reasonably narrow fractions of the benzoate ester of (hydroxypropyl)cellulose (BzPC). They observed that the T_i of this polymer in the bulk sharply increases with increasing M, approaching a limiting temperature T_∞ of 443 K for large M ($M_w > 4 \times 10^5$). This behavior is quite similar to that of THC, and may be interpretable similarly, although the lack of adequate knowledge

about the molecular parameters of BzPC does not allow a quantitative comparison with the theory. Notably, the transition entropy ΔS for high-mass fractions of BzPC was found to be about 0.5 cal/(K·mol of glucose unit). This value is less than half that observed for THC and is perhaps interpretable without introducing the hypothesis of side chain ordering. In fact, the side chain structure of BzPC is obviously less regular and less flexible than that of THC.

Conclusions

The molecular and thermotropic properties of THC were characterized by using narrow fractions of the polymer covering a wide range of molecular weight. The transition temperature T_i depended on chain length in a characteristic fashion. The dependence was adequately interpreted by the previously developed theory, which led to the conclusion that the thermotropicity of this system originates essentially in the temperature-dependent flexibility of the polymer. Thus this work has reinforced from a new angle the idea of Krigbaum, Ciferri, and co-workers[1] about the origin of thermotropicity of semiflexible polymers. The transition entropy ΔS also showed a characteristic dependence on chain length. The comparison with the theory suggested that at least an important portion of ΔS originates in the conformational change of THC. The possibility of the alkyl side chains to order in the mesophase to some extent was also suggested.

References and Notes

(1) (a) Krigbaum, W. R.; Brelsford, G.; Ciferri, A. *Macromolecules* **1989**, *22*, 2487. (b) Ciferri, A. In *Liquid Crystallinity in Polymers*; Ciferri, A., Ed.; VCH Publishers: New York, 1991; Chapter 6.
(2) Part 4: Fukuda, T.; Takada, A.; Tsujii, Y.; Miyamoto, T. *Macromolecules* **1995**, *28*.
(3) Takada, A.; Fukuda, T.; Miyamoto, T.; Watanabe, J. *Cell. Chem. Technol.* **1990**, *24*, 693.
(4) Yamagishi, T. Ph.D. Dissertation, Kyoto University, 1989.
(5) (a) Isogai, A.; Ishizu, I.; Nakano, J. *J. Appl. Polym. Sci.* **1985**, *30*, 345. (b) Yamagishi, T.; Fukuda, T.; Miyamoto, T.; Watanabe, J. *Mol. Cryst. Liq. Cryst.* **1989**, *172*, 17.
(6) Kondo, T.; Gray, D. G. Book of Abstracts; IUPAC MACRO90 (Montreal), 1990; Session 1.8.5.
(7) Dezelic, D.; Vavra, J. *Croat. Chem. Acta* **1966**, *38*, 35.
(8) Koseki, T.; Fukuda, T.; Kitabatake, N.; Doi, E. *Food Hydrocoll.* **1989**, *3*, 135.
(9) Yamakawa, H.; Fujii, M. *Macromolecules* **1974**, *7*, 128.
(10) Yamakawa, H.; Yoshizaki, T. *Macromolecules* **1980**, *13*, 633.
(11) Tsuji, T.; Norisuye, T.; Fujita, H. *Polym. J.* **1975**, *7*, 558.
(12) Fujii, K.; Fukuda, T. Unpublished experiment.
(13) Jones, D. W. *J. Polym. Sci.* **1958**, *32*, 371.
(14) Yoshizaki, T.; Nitta, I.; Yamakawa, H. *Macromolecules* **1988**, *21*, 165.
(15) Benoit, H.; Doty, P. *J. Phys. Chem.* **1953**, *57*, 958.
(16) Bushin, S. V.; Tsvetkov, V. N.; Lysenko, E. B.; Emelyanov, V. N. *Vysokomol. Soedin.* **1981**, *A23*, 2494.
(17) Bohdanecký, M. *Macromolecules* **1983**, *16*, 1483.
(18) Norisuye, T.; Fujita, H. *Polym. J.* **1982**, *14*, 143.
(19) Fukuda, T.; Tsujii, Y.; Koseki, T.; Kitabatake, N.; Doi, E. *Macromolecules* **1991**, *24*, 6786.
(20) (a) Kamide, K.; Saito, M. *Adv. Polym. Sci.* **1987**, *83*, 1. (b) Brelsford, G. L.; Krigbaum, W. R. In *Liquid Crystallinity in Polymers*; Ciferri, A., Ed.; VCH Publishers: New York, 1991; Chapter 2.
(21) Danhelka, J.; Netopilik, M.; Bohdanecký, M. *J. Polym. Sci., Polym. Phys.* **1987**, *25*, 1801.
(22) Meyerhoff, G. *J. Polym. Sci.* **1958**, *29*, 399.
(23) Brant, D. A.; Goebel, K. D. *Macromolecules* **1972**, *5*, 536.
(24) Flory, P. J. *Proc. R. Soc. London* **1956**, *234*, 60 & 73.
(25) Yamagishi, T.; Fukuda, T.; Miyamoto, T.; Watanabe, J. *Mol. Cryst. Liq. Cryst.* **1989**, *172*, 17.
(26) Saito, N.; Takahashi, K.; Yunoki, Y. *J. Phys. Soc. Jpn.* **1967**, *22*, 219.
(27) Fukuda, T.; Takada, A.; Miyamoto, T. *Macromolecules* **1991**, *24*, 6210.
(28) Fukuda, T.; Kawabata, K.; Tsujii, Y.; Miyamoto, T. *Macromolecules* **1992**, *25*, 2196.
(29) Kawabata, K.; Fukuda, T.; Tsujii, Y.; Miyamoto, T. *Macromolecules* **1993**, *26*, 3980.
(30) Bhadani, S. N.; Gray, D. G. *Makromol. Chem., Rapid Commun.* **1982**, *3*, 449.

MA9460854